



# Preparation and evaluation of the electrocatalytic activity of PEMFC electrodes with highly efficient Pt utilization and without ionomer addition



M.C. Campagnolo, C.A. Marozzi, A.C. Chialvo, M.R. Gennero de Chialvo\*

Programa de Electroquímica Aplicada e Ingeniería Electroquímica (PRELINE), Facultad de Ingeniería Química, Universidad Nacional del Litoral, Santiago del Estero 2829, Santa Fe, Argentina

## HIGHLIGHTS

- Preparation of PEMFC electrodes with highly efficient Pt utilization.
- Pulsed electrodeposition of Pt on commercial porous carbon substrates.
- Design of a special cell for both preparation and evaluation of electrodes.
- Electrocatalytic activities for hydrogen oxidation and oxygen reduction.

## ARTICLE INFO

### Article history:

Received 17 December 2012

Received in revised form

23 February 2013

Accepted 20 March 2013

Available online 1 April 2013

### Keywords:

Proton exchange membrane fuel cell

Gas diffusion electrodes

Low platinum loading

Pulsed electrodeposition

## ABSTRACT

A simple method for the preparation of electrodes for proton exchange membrane fuel cell (PEMFC) is proposed, based on the electrodeposition of Pt on commercial porous carbon substrates from  $\text{H}_2\text{SO}_4$  solutions with small amounts of  $\text{H}_2\text{PtCl}_6$ . A special electrochemical cell was designed and built for this purpose, which enables both the preparation and the subsequent evaluation of the obtained electrodes. The electrocatalytic activities for the hydrogen oxidation (HOR) and for the oxygen reduction reaction (ORR) were determined and compared with those of commercial electrodes. Some of the electrodes prepared by the proposed method, with much less platinum loadings and no ionomer addition to the active layer, showed performances similar or higher than those of commercial electrodes. In particular, an outstanding behaviour was obtained with the substrate E-Tek GDL carbon cloth, where the electrodeposition was carried out on the microporous side.

© 2013 Elsevier B.V. All rights reserved.

## 1. Introduction

In the searching for less contaminant and more efficient methods for energy conversion, fuel cells are promising devices, nowadays under intensive research [1,2]. In particular the proton exchange, or polymer electrolyte, membrane fuel cell (PEMFC) combines a series of interesting features such as high energy density, low temperature operation, long stack life and fast start-up, which make them suitable for stationary and portable applications, with either low or high power requirements [3–6]. Nevertheless, some economical and technical challenges must be overcome before getting their wide massive commercialization. Among them, the electrodes fabrication constitutes an important factor in the total PEMFC cost, taking into account that platinum

still remains as one of the best electrocatalysts for both the anode and the cathode [7,8].

In this context, many efforts have been done in order to reduce the Pt loading in PEMFC electrodes [9,10]. Different techniques were employed for this goal, such as electroless deposition [11], thin-film method [12], sputter deposition [13], gamma irradiation [14], supercritical deposition [15], hydrothermal method [16], dual ion-beam assisted deposition [17], etc. In particular, metal electrodeposition is able to become a simple and cheap method to obtain electrodes with low Pt loadings, having many degrees of freedom originated in the numerous variables that can be manipulated (as electrolytic solution composition, temperature, type of electrical signal, time of application, etc.) [18,19]. In particular, pulsed electrodeposition allows maintaining a higher average concentration of the metallic ion nearby the electrode–solution interface and enables a better control of metal particle size [20,21].

Several authors have taken advantage of electrodeposition characteristics for obtaining metal nanoparticles deposited on

\* Corresponding author. Tel.: +54 342 4571164x2519; fax: +54 342 4536861.  
E-mail address: [mchialvo@fiq.unl.edu.ar](mailto:mchialvo@fiq.unl.edu.ar) (M.R. Gennero de Chialvo).

various substrates, looking for a more efficient utilization of expensive electrocatalysts. Some of them studied the electrodeposition of metals on compact carbon substrates (glassy carbon, HOPG, etc.), often coated with a conductor polymer, in order to find conditions for improving the metal dispersion, the three-phases contact, etc. [19,22,23]. In other cases, the electrodeposition process was directly conducted on porous carbon substrates (as carbon powder pastes, carbon papers, carbon clothes, carbon nanotubes, etc.). The porous carbon has not been usually used as purchased, but it has been subjected to one or more previous treatments with the purpose, as a general concept, of activating its surface in order to improve the electrodeposition process. It could be a chemical treatment [24–27] or the application of cyclic voltammetry [24,28] to promote the formation of specific superficial chemical groups or a particular morphology. In other cases, some additives were added to the electrolytic solution [29–31] or ultrasound was used [32,33] to influence the electrodeposition process.

Another common way to try enhancing the surface properties was the addition of hydrophobic and hydrophilic layers to the porous carbon substrate in order to control the thickness of the electrode active layer and improve the utilization of the electrocatalyst [34,35]. It is likely that, even for the thinnest hydrophilic layer, the electrocatalyst particles deposited inside a microporous carbon structure are much more inefficient than those located on its outermost surface, due to the current distribution problems which inevitably arise into a highly porous structure. Therefore, metal particles should be deposited only on the most exterior surface of the substrate. Thus, the use of commercial carbon substrates with no previous activating treatments should avoid the penetration of the electrodeposition solution into the porous structure, due to their natural hydrophobicity.

In this context, the present work proposes a simple method for the preparation of PEMFC electrodes, by square wave galvanostatic pulsed electrodeposition of Pt on different commercial microporous carbon substrates, in  $\text{H}_2\text{SO}_4$  solutions containing small amounts of  $\text{H}_2\text{PtCl}_6$ . The apparent electrocatalytic activities for the hydrogen oxidation reaction (HOR) and for the oxygen reduction reaction (ORR) are determined in order to find electrodeposition conditions for obtaining electrodes with high performances for these two PEMFC reactions and simultaneously with low Pt loadings. Moreover, the performance of these electrodes is compared with that of commercial electrodes.

## 2. Experimental

### 2.1. Electrochemical cell

A special three-electrodes electrochemical cell (Fig. 1) was designed and built in order to carry out both, the preparation and the subsequent evaluation of the obtained electrodes. It consists of a cylindrical glass vessel that contains the electrolytic solution and with a Teflon cap, which holds the counterelectrode, the reference electrode and the gas bubbling tube. The lower part of the main glass vessel, with lesser diameter, is placed inside a cylindrical body, which consists of three pieces. The working electrode is put between the upper Teflon piece and the intermediate graphite piece (which enables the electrical connection). The lower Teflon piece contains three tubes for the input and output of the flowing gases in order to get a homogeneous gas distribution. These three pieces are strongly pressed by means of four metal screwed rods with washers and nuts. Thus the working electrode is in close contact with both, the electrolytic solution through its superior face and the flowing gas by its inferior face, keeping at the same time a high tightness between the different parts. This special cell has also the advantage of allowing the electrode preparation and its

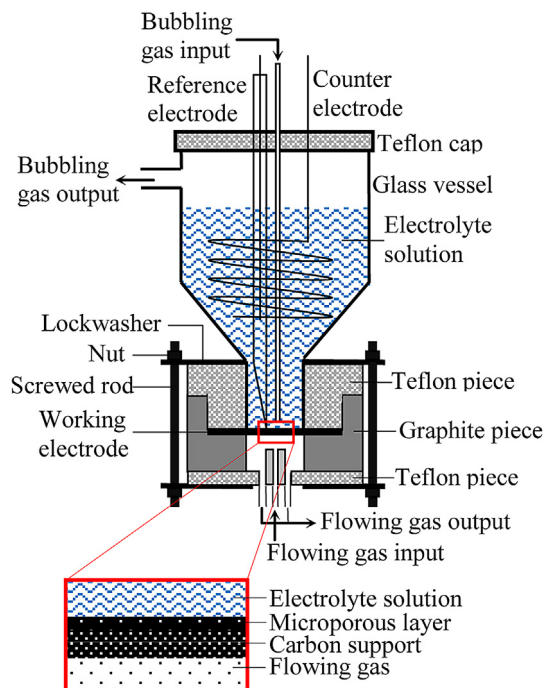


Fig. 1. Simplified scheme of the special three-electrodes electrochemical cell.

subsequent electrochemical evaluation without disassembling the cell, but changing the electrolytic solution and the flowing gas, which is practical and quick. The geometric area of the working electrode exposed to the electrolytic solution and to the flowing gas was  $0.385 \text{ cm}^2$ . A slight overpressure ( $\sim 2 \text{ cm}$  water) of the flowing gas was applied under the working electrode so as it penetrated inside the porous structure and diffused into the electrolyte solution, but did not bubble through it. Thus, the electrode behaviour resembled that of a real fuel cell.

### 2.2. Electrodes preparation

Three different commercial carbon papers, AvCarb P75T, AvCarb GDS2120 and Toray TGP-H-120, provided by Fuel Cell Store, and a carbon cloth with a gas diffusion layer (GDL) on one side (E-Tek) were used as substrates. AvCarb P75T is a carbon particle-filled, polyacrylonitrile (PAN) based carbon fiber paper. AvCarb GDS2120 is based on the previous one and then coated with a microporous layer for the control of permeability, diffusivity and conductivity. Toray TGP-H-120 is a Teflon treated carbon fiber paper. The Teflon gives the carbon material more hydrophobic properties. Finally, the E-Tek GDL consists of a woven fabric with a microporous layer on one side, characterized by the extremely dissimilar surface topography between both sides. The surface morphologies of these substrates were observed by scanning electron microscopy (SEM) and are shown in Fig. 2.

On the other hand, two commercial PEMFC electrodes were used as standard comparison for the electrodeposited electrodes. They were ELAT GDE LT 120E-W ( $0.5 \text{ mg Pt cm}^{-2}$ , 30% Pt/Vulcan XC-72R, support: carbon cloth), provided by Fuel Cell Store and EC-10-05-7 ( $0.5 \text{ mg Pt cm}^{-2}$ , 10% Pt/Vulcan XC-72, support: carbon paper), provided by ElectroChem Inc. These two electrodes are quite representative of the present state of the art, as their carbon supports and their Pt loading are usual at commercial PEMFC electrodes fabrication.

The Pt electrodeposition process was carried out in  $\text{H}_2\text{SO}_4$  solutions with concentrations ( $C_{\text{H}_2\text{SO}_4}$ ) ranging from 0.01 to 1 M, and  $\text{H}_2\text{PtCl}_6$  with concentrations ( $C_{\text{H}_2\text{PtCl}_6}$ ) ranging between  $10^{-5}$  and

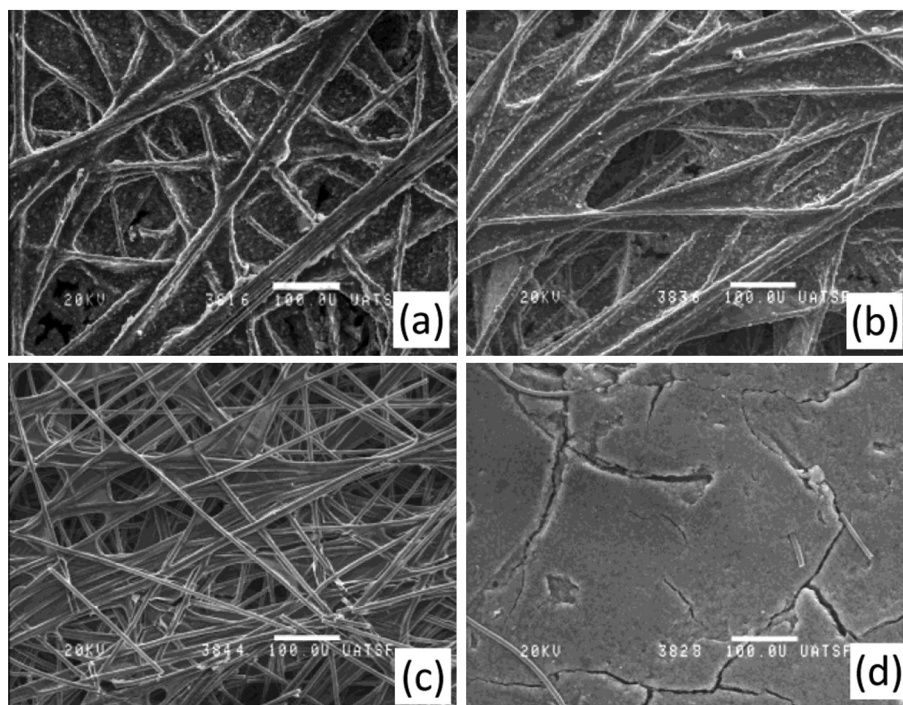


**Fig. 2.** SEM micrograph of the carbon substrates. (a) AvCarb GDS2120, (b) AvCarb P75T, (c) Toray TGP-H-120, (d) E-Tek GDL carbon cloth (microporous side). Magnification: 200 $\times$ .

$10^{-3}$  M. All the electrolytic solutions were prepared with pro-analysis reactants (Merck) and with bi-distilled water, which was then treated in a purifier Elga Purelab. The electrochemical cell was controlled by a Bank Elektronik Wenking POS 2 potentiostat-galvanostat, commanded by an Advantech PCI1710HG D/A board and the software LabView 6i. All the experiments were carried out at 25  $^{\circ}$ C.

The counterelectrode was a high geometric area helical Pt wire and the reference electrode was a reversible hydrogen electrode in the same medium, placed in a Luggin-Haber capillary, which was put very close ( $<0.5$  mm) to the upper surface of the working electrode. All the potentials ( $E$ ) informed in this work are respect to this reference electrode.

The electrodeposition process was carried out through the application of square wave galvanostatic pulses, where the wave period ( $t_p$ ) was varied in the interval from 70  $\mu$ s to 0.5 s, and the total time ( $t_t$ ) was ranged from 1 to 4 h. The deposition current density ( $j_d$ ), related to the geometric area, was varied from 10 to 600 mA cm $^{-2}$  and was applied during the time  $t_{on}$ , while the rest of the square wave period (time  $t_{off}$ ) was at zero current. Meanwhile, the active reduction fraction of the square wave period ( $f_{on} = t_{on}/t_p$ ) was varied from 0.1 to 0.5. Furthermore, all experiments were carried out under N $_2$  bubbling near the upper surface of the electrode, in order to agitate the solution and improve the mass transport.

The electrodes obtained by pulsed electrodeposition were characterized morphologically by scanning electron microscopy (SEM) and electrochemically by cyclic voltammetry.

### 2.3. Apparent electrocatalytic activity

The apparent electrocatalytic activity, measured as the current density per geometric electrode area ( $j_g$ ), of the electrodes obtained as described above was determined for both, the hydrogen oxidation reaction (HOR) and the oxygen reduction reaction (ORR). Measurements of the polarization curves  $j_g$  vs.  $E$  were

carried out in the same cell where the electrodes were obtained, in 0.5 M H $_2$ SO $_4$  solution with the reactant gas (H $_2$  or O $_2$ ) flowing from the inferior side of the electrode, through the application of a slow potentiodynamic sweep run at  $10^{-3}$  V s $^{-1}$ . The HOR was evaluated in the potential range from 0 to 0.2 V while ORR was determined in the potential range comprised between 0.5 and 1.2 V.

### 2.4. Mass electrocatalytic activity

The mass content of the electrodeposited Pt on the carbon substrates was calculated from the difference between the concentration C $_{H_2PtCl_6}$  in the electrolytic solution before and after the electrodeposition, determined by means of a Perkin Elmer 3110 atomic absorption spectrometer. This evaluation was carried out for the electrodes with better apparent electrocatalytic activity. The efficiency in the utilization of the Pt electrocatalyst was estimated through the evaluation of the mass electrocatalytic activity ( $a_m$ ) of the HOR and the ORR, which were determined by the current per Pt mass unit, calculated dividing  $j_g$  by the Pt mass per unit of geometric electrode area ( $m_{Pt}$ ).

## 3. Results and discussion

### 3.1. Electrode characterization

The surface morphology of the Pt electrodeposits was analysed through SEM observations. Fig. 3 illustrates the micrographs of the electrodes prepared on the four types of carbon substrates. They correspond to the following electrodeposition conditions: C $_{H_2SO_4}$  = 0.3 M, C $_{H_2PtCl_6}$  =  $1.6 \times 10^{-4}$  M,  $t_t$  = 4 h,  $j_d$  = 0.4 A cm $^{-2}$ ,  $t_p$  = 70  $\mu$ s and  $f_{on}$  = 0.5. In all cases, after electrodeposition, the electrode was rinsed repeatedly with ultra pure water and then subjected to cyclic voltammetry in H $_2$ SO $_4$  0.5 M solution in the same cell with flowing N $_2$  in the potential range from 0.05 to 1.5 V and with a sweep rate of 0.1 V s $^{-1}$ . Fig. 4 illustrates as an example



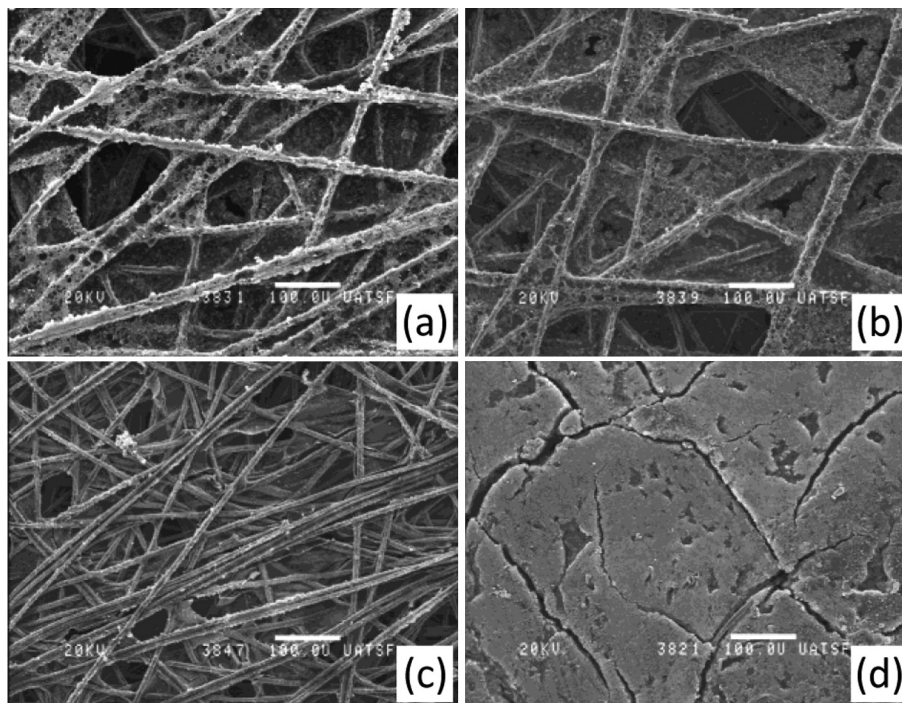


**Fig. 3.** SEM micrograph of the Pt electrodeposits on the carbon substrates. (a) AvCarb GDS2120, (b) AvCarb P75T, (c) Toray TGP-H-120, (d) E-Tek GDL carbon cloth (microporous side). Magnification: 200 $\times$ .

the voltammogram corresponding to the substrate AvCarb GDS2120 carbon paper before (Fig. 4a) and after (Fig. 4b) the electrodeposition carried out in the following conditions:  $C_{H_2SO_4} = 0.3$  M,  $C_{H_2PtCl_6} = 8 \times 10^{-4}$  M,  $t_t = 4$  h,  $j_d = 0.4$  A cm $^{-2}$ ,  $t_p = 70$   $\mu$ s and  $f_{on} = 0.5$ . It can be observed that the voltammogram displays the typical profile corresponding to Pt in acid solutions. Moreover, the Pt electrochemical active surface area was evaluated from these voltammograms, using the area of the hydrogen adsorption region and following the criterion of R.Woods [36], which considers that the hydrogen electroadsorption charge on Pt at 0.06 V represents the 77% of the monolayer charge (161,7  $\mu$ C/cm $^2$ ). It was then expressed as a roughness factor ( $f_r$ ), dividing by the geometric area of the electrode. The respective  $f_r$  values are included in the description of the electrodeposition conditions corresponding to Figs. 6–13 below.

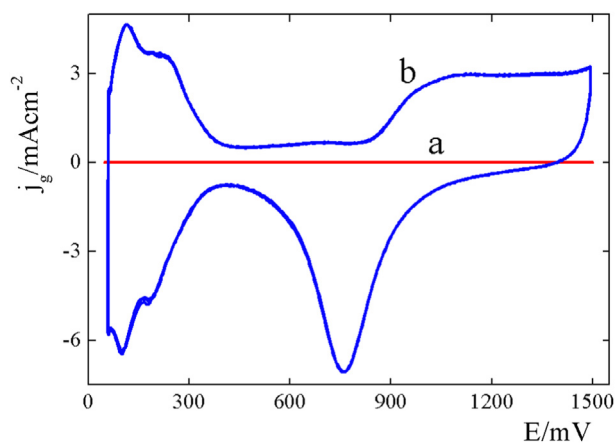


**Fig. 4.** Voltammetric profiles of the AvCarb GDS2120 carbon paper before (a) and after (b) Pt electrodeposition.  $H_2SO_4$  0.5 M, 25  $^{\circ}$ C. Sweep rate: 0.1 V s $^{-1}$ .

### 3.2. Rest potential

Previously to the measurement of the polarization curves for the HOR and ORR, the corresponding rest potentials ( $E_r$ ) under  $H_2$  or  $O_2$  flowing respectively, were recorded as a function of time ( $t$ )

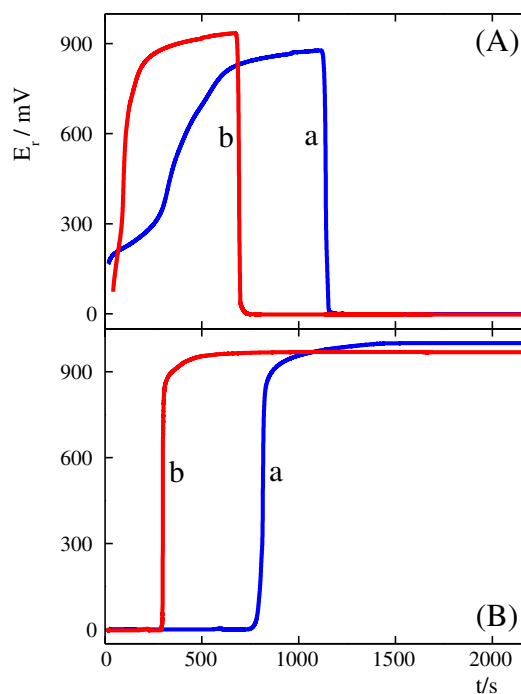


**Fig. 5.** Rest potential vs. time for two electrodes (a, b) prepared at different electro-deposition conditions (described in the text) with circulation of  $H_2$  (A) and  $O_2$  (B).  $H_2SO_4$  0.5 M, 25  $^{\circ}$ C.

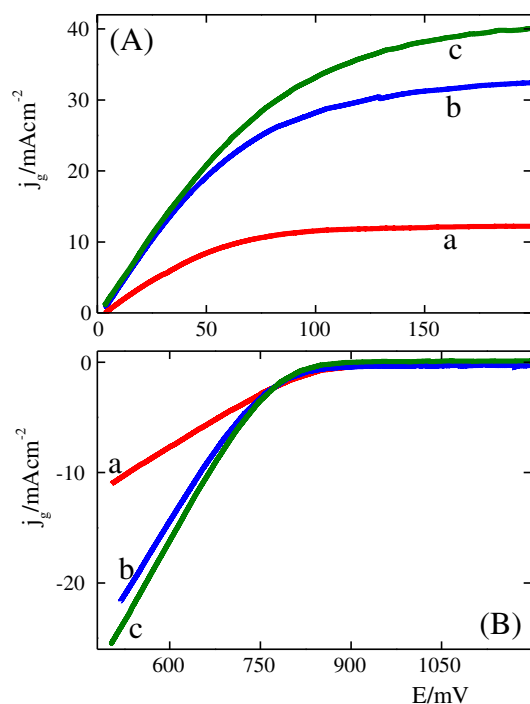


**Fig. 6.** Polarization curves for (A) HOR and (B) ORR of Pt/C electrodes obtained by electrodeposition on different carbon papers: (a) Toray TGP-H-120, (b) AvCarb P75T, (c) AvCarb GDS2120. H<sub>2</sub>SO<sub>4</sub> 0.5 M, 25 °C.

until a constant value was obtained. In the case of H<sub>2</sub> experiment, when finishing the cyclic voltammetry and stopping the N<sub>2</sub> flow, the  $E_r$  began increasing slowly until H<sub>2</sub> flow started. At that time, the  $E_r$  abruptly fell down and always reached the equilibrium value

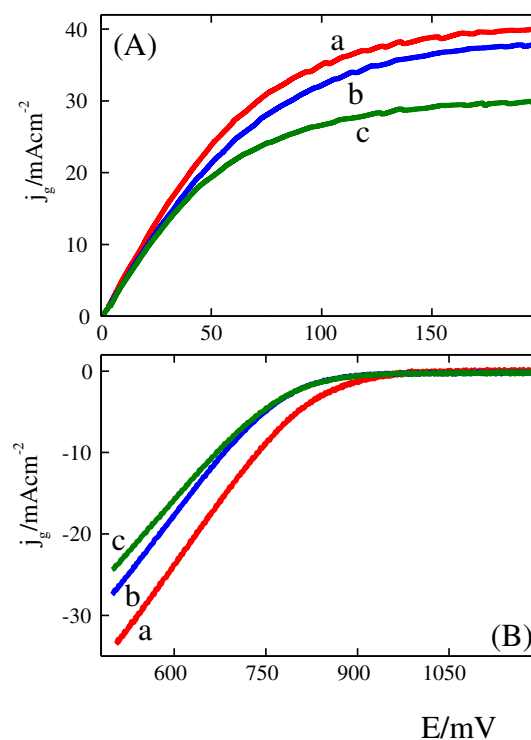


**Fig. 8.** Polarization curves for (A) HOR and (B) ORR of Pt/C electrodes obtained by electrodeposition at different H<sub>2</sub>SO<sub>4</sub> concentrations: (a) 0.05 M, (b) 0.3 M, (c) 0.5 M H<sub>2</sub>SO<sub>4</sub> 0.5 M, 25 °C.

corresponding to the hydrogen electrode reaction (HER). On the other hand, when H<sub>2</sub> was substituted by O<sub>2</sub>, the  $E_r$  increased until reaching a value near 1 V. As it is known, the equilibrium potential corresponding to the oxygen electrode reaction (OER) is not

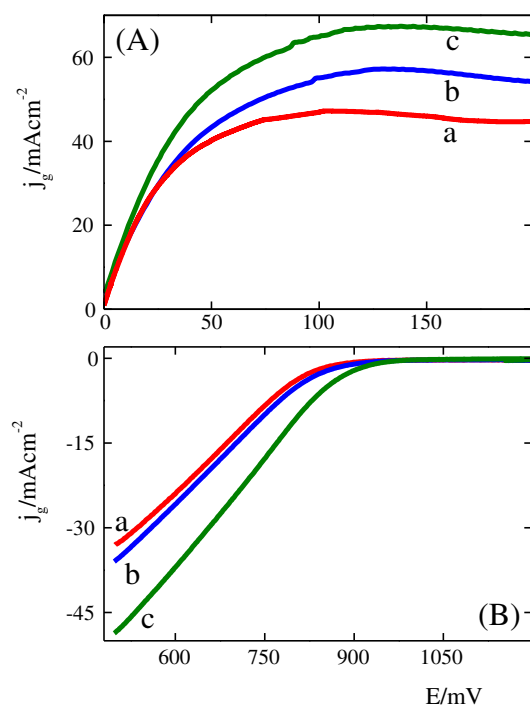


**Fig. 7.** Polarization curves for (A) HOR and (B) ORR of Pt/C electrodes obtained by electrodeposition at different H<sub>2</sub>PtCl<sub>6</sub> concentrations: (a)  $1.6 \times 10^{-4}$  M, (b)  $4.8 \times 10^{-4}$  M, (c)  $8 \times 10^{-4}$  M H<sub>2</sub>SO<sub>4</sub> 0.5 M, 25 °C.

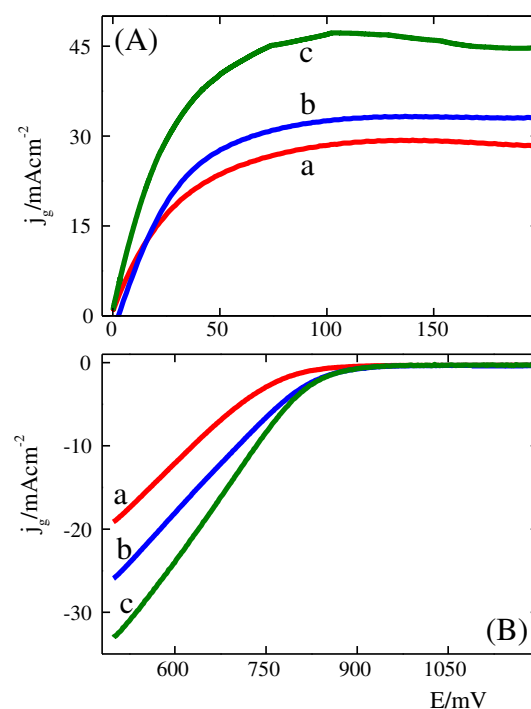


**Fig. 9.** Polarization curves for (A) HOR and (B) ORR of Pt/C electrodes obtained by electrodeposition at different total times: (a) 1 h, (b) 3 h, (c) 4 h H<sub>2</sub>SO<sub>4</sub> 0.5 M, 25 °C.

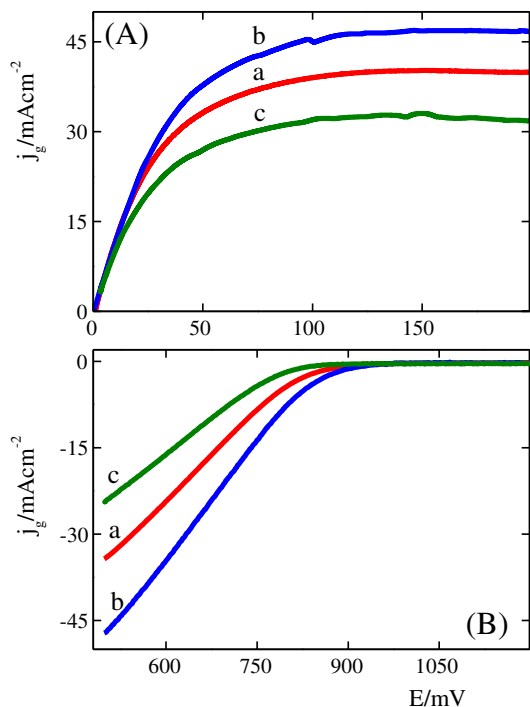


**Fig. 10.** Polarization curves for (A) HOR and (B) ORR of Pt/C electrodes obtained by electrodeposition at different geometric current densities: (a)  $0.05 \text{ A cm}^{-2}$ , (b)  $0.2 \text{ A cm}^{-2}$ , (c)  $0.6 \text{ A cm}^{-2}$ .  $\text{H}_2\text{SO}_4$   $0.5 \text{ M}$ ,  $25^\circ\text{C}$ .

reached due to the existence of secondary reactions, such as PtO formation [37,38]. Examples of the open circuit potential curves are given in Fig. 5A ( $\text{H}_2$ ) and Fig. 5B ( $\text{O}_2$ ) for electrodes obtained on AvCarb GDS2120 substrate and two sets of the electrodeposition

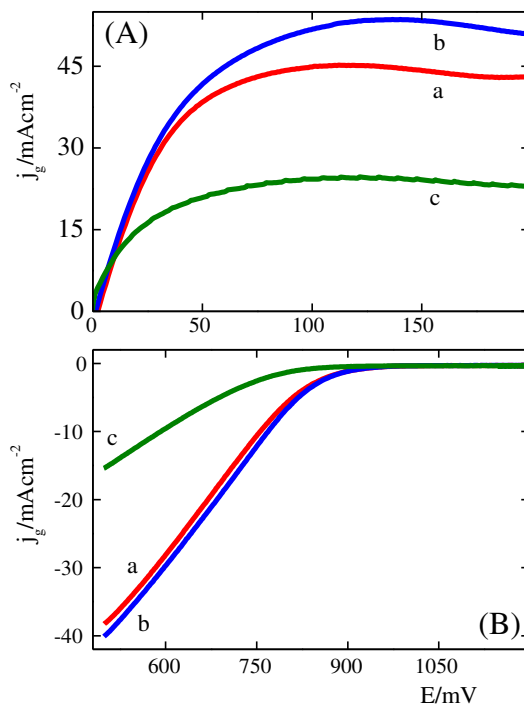


**Fig. 12.** Polarization curves for (A) HOR and (B) ORR of Pt/C electrodes obtained by electrodeposition at different active fractions of the square wave pulse: (a) 0.1, (b) 0.2, (c) 0.4.  $\text{H}_2\text{SO}_4$   $0.5 \text{ M}$ ,  $25^\circ\text{C}$ .

conditions: a)  $\text{C}_{\text{H}_2\text{SO}_4} = 0.05 \text{ M}$ ,  $\text{C}_{\text{H}_2\text{PtCl}_6} = 10^{-3} \text{ M}$ ,  $t_t = 4 \text{ h}$ ,  $j_d = 0.3 \text{ A cm}^{-2}$ ,  $t_p = 0.3 \text{ s}$ ,  $f_{\text{on}} = 0.3$  and b)  $\text{C}_{\text{H}_2\text{SO}_4} = 0.3 \text{ M}$ ,  $\text{C}_{\text{H}_2\text{PtCl}_6} = 3.2 \times 10^{-4} \text{ M}$ ,  $t_t = 4 \text{ h}$ ,  $j_d = 0.4 \text{ A cm}^{-2}$ ,  $t_p = 40 \text{ ms}$ ,  $f_{\text{on}} = 0.1$ .

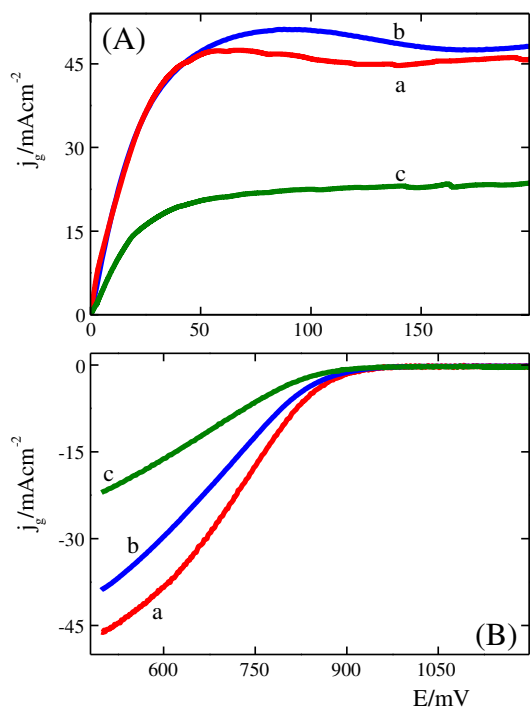


**Fig. 11.** Polarization curves for (A) HOR and (B) ORR of Pt/C electrodes obtained by electrodeposition at different period times of the square wave pulse: (a)  $70 \mu\text{s}$ , (b)  $4 \text{ ms}$ , (c)  $0.4 \text{ s}$ .  $\text{H}_2\text{SO}_4$   $0.5 \text{ M}$ ,  $25^\circ\text{C}$ .

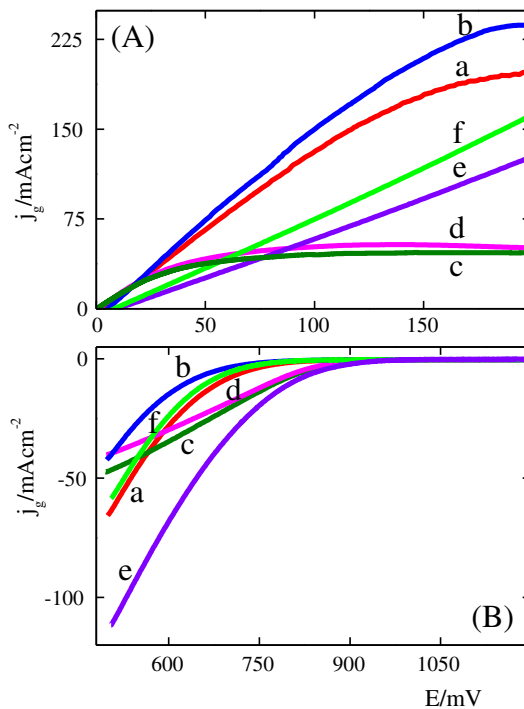


**Fig. 13.** Polarization curves for (A) HOR and (B) ORR. (a–d) Pt/C electrodes prepared at different electrodeposition conditions (described in the text); (e, f) Commercial electrodes.  $\text{H}_2\text{SO}_4$   $0.5 \text{ M}$ ,  $25^\circ\text{C}$ .

It can be appreciated in Fig. 5A that the hydrogen flow on the bottom side of the working electrode produces immediately a potential decrease, reaching the reversible potential yet in absence of bubbling  $H_2$  gas in the electrolyte solution. Then, as  $H_2$  is substituted by  $O_2$ , a sudden increase of potential is produced until the achievement of the mixed potential value characteristic of Pt electrodes in the presence of oxygen [37,38]. This fast response of the rest potential in the presence of the incoming reactant gases can be considered an additional evidence of the right operation of these electrodes in the special electrochemical cell designed.

### 3.3. Apparent electrocatalytic activity

The polarization curves  $j_g$  vs.  $E$  of the Pt/C electrodes for both the hydrogen oxidation and the oxygen reduction reactions were evaluated for different values of the electrodeposition parameters. This study was carried out in order to determine the influence of each parameter on both the preparation process and the performance. Therefore, they were varied one by one, maintaining the others constant. However, taking into account that seven variables can be modified (substrate,  $C_{H_2PtCl_6}$ ,  $C_{H_2SO_4}$ ,  $t_t$ ,  $j_d$ ,  $t_p$ ,  $f_{on}$ ) the combinations of their values lead to an enormous number of possible experiments to be done (for example, with 4 values for every variable, 16384 combinations are obtained). Thus, in this work more than two hundred experiments were carried out, combining those parameters values that were previously considered more significant (based on preliminary experiences). Some of these combinations, where the effect is more marked, are described below. Accordingly, it should be bear in mind that these results are strictly valid for their particular electrodeposition conditions.

#### 3.3.1. Substrate

An example of the change of the substrate is illustrated in Fig. 6, where it is shown the polarization curves corresponding to the HOR (Fig. 6A) and to the ORR (Fig. 6B). The curves correspond to the Pt/C electrodes obtained by electrodeposition carried out in the same conditions on the three different carbon paper substrates. The electrodeposition conditions were  $C_{H_2SO_4} = 0.3$  M,  $C_{H_2PtCl_6} = 10^{-3}$  M,  $t_t = 1$  h,  $j_d = 0.3$  A cm $^{-2}$ ,  $t_p = 0.3$  s and  $f_{on} = 0.1$  ( $f_r$ : (a) 22.99, (b) 11.02, (c) 12.41). It can be observed that current densities for both reactions increase in this case in the order  $j_g(\text{AvCarb GDS2120}) > j_g(\text{AvCarb P75T}) > j_g(\text{Toray TGP-H-120})$ . As the carbon paper AvCarb GDS2120 showed better performances than the other two carbon papers in all the experiments, the other studies were mainly carried out on this carbon paper.

#### 3.3.2. $H_2PtCl_6$ concentration

The variation of the concentration of chloroplatinic acid was studied in this case maintaining the following electrodeposition conditions constant: substrate AvCarb GDS2120 carbon paper,  $C_{H_2SO_4} = 0.3$  M,  $t_t = 4$  h,  $j_d = 0.4$  A cm $^{-2}$ ,  $t_p = 70$   $\mu$ s and  $f_{on} = 0.5$  ( $f_r$ : (a) 7.98, (b) 16.30, (c) 36.11). Fig. 7 shows the polarization curves corresponding to the HOR (Fig. 7A) and to the ORR (Fig. 7B) obtained with the following  $H_2PtCl_6$  concentrations: (a)  $1.6 \times 10^{-4}$  M, (b)  $4.8 \times 10^{-4}$  M, (c)  $8 \times 10^{-4}$  M. As it would be expected in principle, an increase of  $C_{H_2PtCl_6}$  produces an enhancing of the current densities of both reactions.

#### 3.3.3. $H_2SO_4$ concentration

It was also analysed the effect of the concentration of the sulphuric acid in the electrodeposition solution. The following variables were kept constant: substrate AvCarb GDS2120 carbon paper,  $C_{H_2PtCl_6} = 10^{-4}$  M,  $t_t = 1$  h,  $j_d = 0.3$  A cm $^{-2}$ ,  $t_p = 0.3$  s and  $f_{on} = 0.3$  ( $f_r$ : (a) 36.80, (b) 14.71, (c) 16.98). Fig. 8 shows the polarization curves corresponding to the HOR (Fig. 8A) and to the ORR (Fig. 8B) obtained

with the following  $H_2SO_4$  concentrations: (a) 0.05 M, (b) 0.3 M, (c) 0.5 M. It can be observed that in this example both HOR and ORR current densities increase as the  $H_2SO_4$  concentration decreases. Nevertheless, it should be taken into account that it cannot be omitted because in such case, as the  $H_2PtCl_6$  concentration is very low, the conductivity of the electrolyte solution becomes too small.

#### 3.3.4. Total time of electrodeposition

Another variable in the electrodeposition process is the total time of application of the square wave galvanostatic pulses  $t_t$ . The polarization curves depicted in Fig. 9 for the HOR (Fig. 9A) and for the ORR (Fig. 9B) respectively, correspond to the following constant electrodeposition conditions: substrate AvCarb GDS2120 carbon paper,  $C_{H_2SO_4} = 0.3$  M,  $C_{H_2PtCl_6} = 1.6 \times 10^{-4}$  M,  $j_d = 0.4$  A cm $^{-2}$ ,  $t_p = 70$   $\mu$ s and  $f_{on} = 0.5$  ( $f_r$ : (a) 3.69, (b) 6.56, (c) 7.98). Three different values of the total time  $t_t$  were used (1, 3 and 4 h) and it can be observed that the current densities of the HER and HOR increase as the time of electrodeposition increases. This result would indicate that all the amount of Pt deposited on the electrode surface through this technique is mostly available as active sites for the electrocatalysis of the reactions under study.

#### 3.3.5. Current density of electrodeposition

Fig. 10 shows the influence of the current density of electrodeposition  $j_d$  on the polarization curves for the HOR (Fig. 10A) and for the ORR (Fig. 10B) respectively. In this case the following electrodeposition conditions were kept constant: substrate AvCarb GDS2120 carbon paper,  $C_{H_2SO_4} = 0.3$  M,  $C_{H_2PtCl_6} = 8 \times 10^{-5}$  M,  $t_t = 4$  h,  $t_p = 4$  ms and  $f_{on} = 0.5$  ( $f_r$ : (a) 9.62, (b) 8.73, (c) 6.58). Meanwhile, the applied  $j_d$  values were 0.05, 0.2 and 0.6 A cm $^{-2}$ . It can be observed that there is a strong effect of this variable on the polarization curves of both reactions. For these particular electrodeposition conditions, the current densities of the electrocatalytic reactions increase with the electrodeposition current density up to a value near 0.3 A cm $^{-2}$  and then begin to decrease. This behaviour could be due to that at high values of  $j_d$  hydrogen evolution becomes significant, leading to a less adherent deposit.

#### 3.3.6. Period time of the current signal

The influence of the period time  $t_p$  of the square wave galvanostatic pulse was studied maintaining the following electrodeposition conditions constant: substrate AvCarb GDS2120 carbon paper,  $C_{H_2SO_4} = 0.3$  M,  $C_{H_2PtCl_6} = 3.2 \times 10^{-4}$  M,  $t_t = 4$  h,  $j_d = 0.4$  A cm $^{-2}$  and  $f_{on} = 0.5$  ( $f_r$ : (a) 15.40, (b) 14.46, (c) 10.08). Fig. 11 shows the polarization curves corresponding to the HOR (Fig. 11A) and to the ORR (Fig. 11B) obtained with the following  $t_p$  values: (a) 70  $\mu$ s, (b) 4 ms, (c) 0.4 s. The polarization curves show in general a better performance for the lower values of the period time.

#### 3.3.7. Active fraction of the current signal

Finally, the influence of the active fraction  $f_{on}$  of the square wave galvanostatic pulse is illustrated in Fig. 12, where it is shown the polarization curves corresponding to the HOR (Fig. 12A) and to the ORR (Fig. 12B). The curves correspond to the Pt/C electrodes obtained by the application of the following electrodeposition conditions: substrate AvCarb GDS2120 carbon paper,  $C_{H_2SO_4} = 0.3$  M,  $C_{H_2PtCl_6} = 1.6 \times 10^{-4}$  M,  $t_t = 4$  h,  $j_d = 0.4$  A cm $^{-2}$  and  $t_p = 40$  ms ( $f_r$ : (a) 10.86, (b) 13.15, (c) 3.29). Three different values of the active fraction  $f_{on}$  were used (0.1, 0.2 and 0.4). It can be observed that in this case the current densities of the HOR and ORR have a small variation for the lower values of this variable, but an important decrease is produced for  $f_{on} = 0.4$ . This result stands out the importance of the application of a pulse electrodeposition technique because as  $f_{on}$  increases and tends to the application of a constant current, the apparent activities of both reactions decrease significantly.

Finally, it is emphasized again that the trends observed in Figs. 6–12 about the influence of every variable on the HOR and ORR polarization curves cannot be generalized to all the possible combinations of the values of the different parameters, as the pulsed electrodeposition is a quite complex process and the different variables probably present a significant interdependence between their effects. Notwithstanding, they can effectively be considered a strong basis for the analysis of the influence of the different variables on the electrocatalytic activity of the Pt electrodeposits.

#### 3.4. Comparison of the apparent electrocatalytic activity of electrodeposited and commercial electrodes

In order to compare the performance of the electrodes obtained in this work with that of commercial electrodes, the corresponding polarization curves for two of them, ELAT GDE LT 120E-W and EC-10-05-7 were measured in the same experimental conditions. As a proton conducting ionomer layer is usually added to the active layer of PEMFC electrodes before assembling the MEA (membrane-electrode assembly) in order to get their best performance, it was decided to carry out the polarization curves of those electrodes with and without the addition of Nafion<sup>®</sup> polymer film. Thus, a Nafion solution 5 %wt in alcohols (Aldrich) was applied by brushing on the two commercial electrodes in order to obtain a loading of 1 mg Nafion per cm<sup>2</sup> of geometric electrode area, and then the solvent was evaporated in a stove at 80 °C overnight. The comparison of the corresponding polarization curves demonstrated that the performances of both commercial electrodes were substantially improved with the addition of the ionomer. For this reason, the comparison of the responses of these electrodes with those prepared in this work was only done with the commercial electrodes covered with the Nafion<sup>®</sup> film.

Taking into account the experimental experience acquired with all the previous studies, different electrodeposition conditions were tested in order to try obtaining electrodes with high performances for the HOR and for the ORR and thus some good results were achieved. In particular, the E-Tek GDL substrate showed in general much better performances than the AvCarb GDS2120 carbon paper. Fig. 13 illustrates the polarization curves corresponding to the HOR (Fig. 13A) and to the ORR (Fig. 13B) for the two commercial PEMFC electrodes impregnated with Nafion<sup>®</sup> and for some of the electrodeposited Pt/C electrodes without any ionomer addition to their active layers. The selected electrodes were obtained by the application of the following electrodeposition conditions: (a) substrate E-Tek GDL carbon cloth (microporous side),  $C_{H_2SO_4} = 0.3$  M,  $C_{H_2PtCl_6} = 1.6 \times 10^{-4}$  M,  $t_t = 4$  h,  $j_d = 0.4$  A cm<sup>-2</sup>,  $t_p = 70$   $\mu$ s and  $f_{on} = 0.5$  ( $f_r$ : (a) 5.13); (b) substrate E-Tek GDL carbon cloth (microporous side),  $C_{H_2SO_4} = 0.3$  M,  $C_{H_2PtCl_6} = 8 \times 10^{-5}$  M,  $t_t = 4$  h,  $j_d = 0.4$  A cm<sup>-2</sup>,  $t_p = 40$  ms and  $f_{on} = 0.2$  ( $f_r$ : (b) 2.68); (c) substrate AvCarb GDS2120 carbon paper,  $C_{H_2SO_4} = 0.3$  M,  $C_{H_2PtCl_6} = 8 \times 10^{-5}$  M,  $t_t = 4$  h,  $j_d = 0.2$  A cm<sup>-2</sup>,  $t_p = 4$  ms and  $f_{on} = 0.5$  ( $f_r$ : (c) 8.73); (d) substrate AvCarb GDS2120 carbon paper,  $C_{H_2SO_4} = 0.3$  M,  $C_{H_2PtCl_6} = 1.6 \times 10^{-4}$  M,  $t_t = 4$  h,  $j_d = 0.4$  A cm<sup>-2</sup>,  $t_p = 40$  ms and  $f_{on} = 0.2$  ( $f_r$ : (d) 13.15). They were compared with the following commercial electrodes with Nafion<sup>®</sup> impregnation: (e) ELAT GDE LT 120E-W (0.5 mg Pt cm<sup>-2</sup>, 30% Pt/Vulcan XC-72R, support: carbon cloth) ( $f_r$ : (e) 96.96) and (f) EC-10-05-7 (0.5 mg Pt cm<sup>-2</sup>, 10% Pt/Vulcan XC-72, support: carbon paper) ( $f_r$ : (f) 24.06). It can be observed that several electrodeposited electrodes have current densities  $j_g$  very similar, or even superior, than those corresponding to the commercial ones. These results are quite interesting, taking into account that they were prepared by a simple and cheap method and then used with no ionomer addition.

#### 3.5. Comparison of the mass electrocatalytic activity of electrodeposited and commercial electrodes

It should be bear in mind that the apparent electrocatalytic activity  $j_g$  is a good measure to compare performances of different electrodes, but it does not take into account the electrode Pt loading and in consequence it has little connection with the cost of obtaining such performance. Therefore, from an economic point of view, a more appropriate measure of comparison between different electrodes would be any that considers the real use of the electrocatalyst mass. Thus, the mass electrocatalytic activity ( $a_m$ ) is defined as the current per metal mass unit. Both types of electrocatalytic activity together,  $j_g$  and  $a_m$ , will give a more complete description of the performance of a particular electrode.

As it was described in the previous item, it was possible to obtain electrodes with  $j_g$  values similar, or even superior, to that of the commercial electrodes. However, it should be also important to evaluate the mass electrocatalytic activity, as the use of lesser Pt amounts, implying a more efficient utilization of the metal, is a main goal in the searching for reducing the cost of PEMFCs. Therefore, the mass content of the electrodeposited Pt on the carbon substrates was calculated from the difference between the concentration of H<sub>2</sub>PtCl<sub>6</sub> in the electrolytic solution before and after the electrodeposition, which was determined by atomic absorption spectrometry.

Then, the mass electrocatalytic activity of the HOR and the ORR were determined by the current per Pt mass unit, calculated dividing  $j_g$  by the Pt mass per unit of geometric electrode area ( $m_{Pt}$ ). The determination of the electrodeposited Pt mass was performed for the electrodes with better  $j_g$  (similar or superior to that of the commercial ones).

Among the different types of substrates employed for the preparation of the electrodeposited Pt/C electrodes, the E-Tek GDL carbon cloth (microporous side) has shown the best mass electrocatalytic activity. Therefore, Fig. 14 illustrates the curves  $a_m$  vs.  $E$  for the HOR (Fig. 14A) and for the ORR (Fig. 14B) of the two

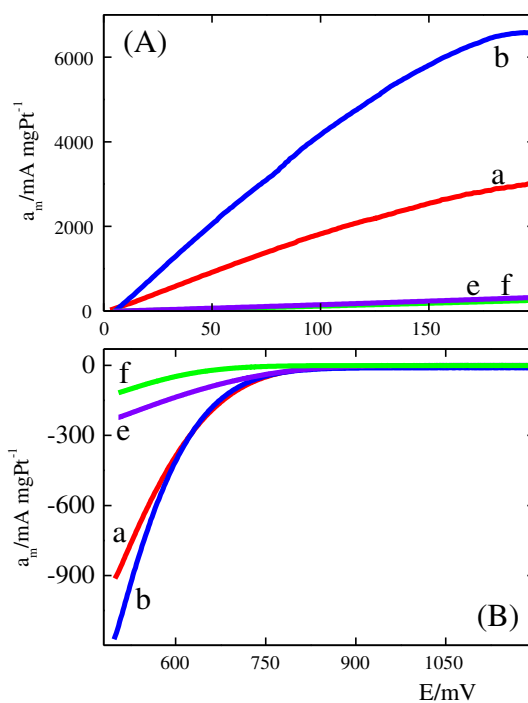


Fig. 14. Mass electrocatalytic activity for (A) HOR and (B) ORR. (a, b) Pt/C electrodes prepared at different electrodeposition conditions (described in the text); (e, f) Commercial electrodes. H<sub>2</sub>SO<sub>4</sub> 0.5 M, 25 °C.



electrodeposited electrodes obtained on this substrate, which polarization curves are shown in Fig. 13 (curves a and b), and they are compared with those corresponding to the commercial electrodes with Nafion® (curves e and f). The real Pt contents of these electrodeposited electrodes were  $0.072 \text{ mg Pt cm}^{-2}$  (a) and  $0.036 \text{ mg Pt cm}^{-2}$  (b), respectively. It can be observed that the mass electrocatalytic activity of these electrodes is significantly higher than that of the commercial electrodes. This advantage is even more important considering that the preparation of these electrodeposits is a rather simple technique, without any pretreatment of the carbon substrate, and the obtained electrodes are later used without any ionomer impregnation of their active layer.

### 3.6. Correlation between the Pt electrochemical active surface area and the HOR and ORR performances

The Pt electrochemical active surface area was evaluated from the corresponding voltammograms in  $\text{H}_2\text{SO}_4$  0.5 M and the result expressed as a roughness factor ( $f_r$ ). In order to determine if the HOR and ORR performances of the different electrodes (electrodeposited and commercial) could be only explained by this Pt electrochemical active surface area, it was decided to correlate both parameters. For this purpose, the maximum values of the current densities of the HOR and ORR within the corresponding overpotential range analysed (that is, at 0.2 V for the HOR and at 0.5 V for the ORR), were taken as representative of the respective electrode performances. These values were expressed as a Pt real

electrocatalytic activity  $j_r$  (that is, real current density per unit of Pt electrochemical active surface area), dividing  $j_g$  by the corresponding roughness factor ( $j_r = j_g/f_r$ ). Both correlations of  $j_r$  versus  $f_r$  are illustrated in Fig. 15A (HOR) and Fig. 15B (ORR). It can be observed that for the electrodes deposited on the substrate AvCarb GDS2120 carbon paper and for the commercial electrodes, the value of the Pt real electrocatalytic activity is quite similar, showing a slight decrease with the increase of the roughness factor. Therefore, in these both cases, the Pt electrochemical active surface area is working in a similar way and the variations in the apparent electrocatalytic activity between different electrodes can be basically assigned to their different Pt roughness. But, on the other hand, the variations in the mass electrocatalytic activity would be originated in a different ratio area/mass of the electrocatalyst.

On the contrary, for the electrodes deposited on the substrate E-Tek GDL carbon cloth (microporous side), the Pt real electrocatalytic activity is much higher than that of the other electrodes and this effect is more pronounced in the case of the HOR. Consequently, in this case the Pt electrochemical active surface area is working much more efficiently and this improvement is really outstanding. So, in this case the variations in the apparent and in the mass electrocatalytic activities cannot be only explained by a different Pt roughness factor or by a different ratio area/mass. Therefore, the much better Pt real electrocatalytic activity for these electrodes would probably be indicating that other factors are influencing the efficiency of the Pt surface (like accessibility of reactants to the surface, current distribution phenomena, local pH variations, etc.), and in turn these factors could be related to the totally different morphology of this substrate with respect to the carbon papers.

## 4. Discussion

Electrodes were prepared for their use in PEMFC cells by a simple and cheap method. This preparation was carried out in a specially designed electrochemical cell and it consisted in the Pt galvanostatic pulsed electrodeposition from diluted precursor solutions on commercial porous carbon substrates employed as purchased. This procedure takes advantage of the natural hydrophobicity characteristics of these substrates to obtain Pt particles deposited on the outermost surface of the substrates, enabling a high utilization of the metal. Furthermore, the use of the carbon substrates without any previous treatment gives greater simplicity, quickness and lower cost than other fabrication methods, which usually have one or more previous steps for activating the substrate surface.

The special electrochemical cell, designed and built for this work, allows the simultaneous contact of the electrode with an electrolytic solution by its upper face and with a flowing gas by its lower face. This design has the additional advantage of enabling the electrode preparation and its subsequent electrochemical evaluation in the same cell, by just changing the electrolytic solution and the flowing gas. Thus, the electrodes can be characterized independently of the polymer membrane and the counterelectrode present in a complete fuel cell, leaving out the uncertainties introduced by the phenomena involved in these two other fuel cell elements.

The electrodes prepared in this cell exhibited a good adherence of Pt to the carbon substrate, since the corresponding voltammograms exhibit the typical profile of the massive Pt in acid medium. In addition, in presence of the incoming reactant gases, the rest potential presents a fast response, reaching the exact equilibrium potential (HOR) or close to it (ORR).

It has been also shown that the change of every electrodeposition variable has some effect on the apparent electrocatalytic activity for the two reactions usually present in a PEMFC, hydrogen

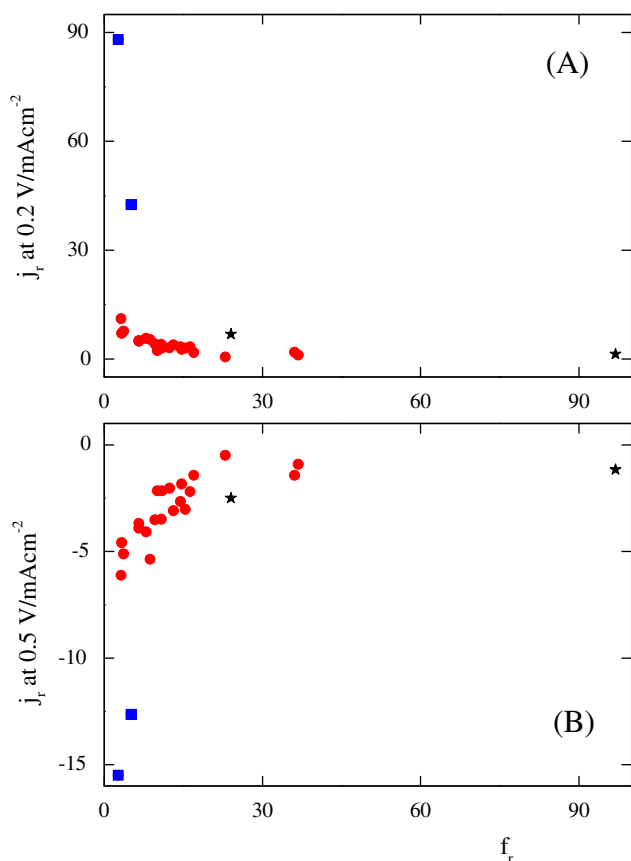


**Fig. 15.** Correlation between the Pt real electrocatalytic activity for (A) HOR and (B) ORR and the Pt roughness factor of the corresponding electrodes (all of them shown in Figs. 6–13 and described in the text). Dots: electrodes deposited on AvCarb GDS2120 carbon paper, squares: electrodes deposited on E-Tek GDL carbon cloth (microporous side), stars: commercial electrodes.

oxidation and oxygen reduction. These experiments indicate that there is certain interdependence between the values of the different electrodeposition variables, so that no absolute conclusions can be drawn about the influence of each variable. Therefore, different electrodeposition conditions were tested with the target of producing electrodes having simultaneously high apparent electrocatalytic activity and high mass electrocatalytic activity, taking into account that both together (rather than each alone) give a more complete description of the electrode performance related to its cost. Some particular combinations of the values of the electrodeposition variables allowed obtaining electrodes with high values of both  $j_g$  and  $a_m$ , that is with a more efficient use of the electrocatalyst mass.

On the other hand, the correlation between the HOR and ORR performances of the obtained electrodes and the Pt electrochemical active surface area has shown a clear difference between the electrodes deposited on the substrate E-Tek GDL carbon cloth (microporous side) with respect to the other electrodes (those deposited on the AvCarb GDS2120 carbon paper and the commercial ones). The Pt electrodeposited on this particular support has shown a noteworthy much higher real electrocatalytic activity (per unit of real Pt surface area) and so indicating that other factors (reactant gases mass transport, current distribution, etc.) are playing a not negligible role on the electrochemical efficiency of this active area.

Furthermore, several electrodeposited electrodes showed similar or even superior apparent electrocatalytic activity and higher mass electrocatalytic activity than two commercial electrodes. Moreover these better performances were reached with no ionomer addition to their active layers. In this sense, it is emphasized the outstanding performances achieved with the Pt electrodeposits obtained on the substrate E-Tek GDL carbon cloth (microporous side), much more superior than those obtained with the other three carbon substrates. This result is striking not only by itself, but because this substrate was used in a way not predicted in principle for it. This GDL carbon cloth is normally designed and fabricated to be used with its microporous side exposed to the gas, not to the electrolyte. A probable reason for this interesting and promising behaviour could be in its morphology, clearly different from that of the studied carbon papers. This significant conduct deserves more research and further studies about the preparation of substrate materials with morphologies similar to this commercial E-Tek GDL are under progress.

## 5. Conclusions

A simple method was developed to produce cheap PEMFC electrodes, consisting in the galvanostatic pulsed electrodeposition from Pt diluted precursor solutions on commercial porous carbon substrates employed as purchased. A special electrochemical cell was designed and built, which was used for both the electrode preparation and its subsequent electrochemical evaluation.

In addition to the advantage of using the carbon substrates with no previous treatments, some of the electrodeposited electrodes exhibited high apparent and mass electrocatalytic activities, with an efficient utilization of the Pt mass, when compared with commercial electrodes. Moreover, these good performances are achieved with no ionomer impregnation of their active layers (to our knowledge, no previous work has prepared PEMFCs electrodes to be used with no ionomer addition).

Finally, it is highlighted the outstanding behaviour reached with the Pt electrodeposits prepared on the substrate E-Tek GDL carbon cloth (microporous side), which exhibit a much higher Pt real electrocatalytic activity.

## Acknowledgements

The authors thank CONICET, ANPCyT and UNL for the financial support.

## References

- [1] S. Srinivasan, *Fuel Cells: From Fundamentals to Applications*, Springer Verlag, New York, 2006.
- [2] S.M. Haile, *Acta Mater.* 51 (2003) 5981–6000.
- [3] V. Mehta, J.S. Cooper, *J. Power Sources* 114 (2003) 32–53.
- [4] J. Zang (Ed.), *PEM Fuel Cell Electrocatalysts and Catalyst Layers. Fundamentals and Applications*, Springer Verlag, London, 2008.
- [5] H. Zhang, P.K. Shen, *Chem. Soc. Rev.* 41 (2012) 2382–2394.
- [6] S. Sharma, B.G. Pollet, *J. Power Sources* 208 (2012) 96–119.
- [7] S. Litster, G. McLean, *J. Power Sources* 130 (2004) 61–76.
- [8] H.A. Gasteiger, S.S. Kocha, B. Sompalli, F.T. Wagner, *Appl. Catal. B Environ.* 56 (2005) 9–35.
- [9] A. Esmaeilifar, S. Rowshanzamir, M.H. Eikani, E. Ghazanfari, *Energy* 35 (2010) 3941–3957.
- [10] J.H. Wee, K.Y. Lee, S.H. Kim, *J. Power Sources* 165 (2007) 667–677.
- [11] K.D. Beard, M.T. Schaal, J.W. Van Zee, J.R. Monnier, *Appl. Catal. B Environ.* 72 (2007) 262–271.
- [12] L. Xiong, A. Manthiram, *Electrochim. Acta* 50 (2005) 3200–3204.
- [13] K.L. Huang, Y.C. Lai, C.H. Tsai, *J. Power Sources* 156 (2006) 224–231.
- [14] D.F. Silva, A. Oliveira Neto, E.S. Pino, M. Linardi, E.V. Spinace, *J. Power Sources* 170 (2007) 303–307.
- [15] A. Bayrakceken, A. Smirnova, U. Kitkamthorn, M. Aindow, L. Turker, I. Eroglu, C. Erkey, *J. Power Sources* 179 (2008) 532–540.
- [16] L. Chen, G. Lu, *Electrochim. Acta* 53 (2008) 4316–4323.
- [17] M.S. Saha, A.F. Gulla, R.J. Allen, S. Mukerjee, *Electrochim. Acta* 51 (2006) 4680–4692.
- [18] Z.D. Wei, S.H. Chan, L.L. Li, H.F. Cai, Z.T. Xia, C.X. Sun, *Electrochim. Acta* 50 (2005) 2279–2287.
- [19] M.M.E. Duarte, A.S. Pilla, J.M. Sieben, C.E. Mayer, *Electrochem. Commun.* 8 (2006) 159–164.
- [20] S.M. Ayyadurai, Y.S. Choi, P. Ganesan, S.P. Kumaraguru, B.N. Popov, *J. Electrochem. Soc.* 154 (2007) B1063–B1073.
- [21] F. Alcaide, G. Álvarez, J.A. Blázquez, P.L. Cabot, O. Miguel, *Int. J. Hydrogen Energy* 35 (2010) 5521–5527.
- [22] A.A. Mikhaylova, O.A. Khazova, V.S. Bagotzky, *J. Electroanal. Chem.* 480 (2000) 225–232.
- [23] J.L. Zubimendi, L.V.ázquez, P. Ocón, J.M. Vara, W.E. Triaca, R.C. Salvarezza, A.J. Arvia, *J. Phys. Chem.* 97 (1993) 5095–5102.
- [24] H. Tang, J.H. Chen, Z.P. Huang, D.Z. Wang, Z.F. Ren, L.H. Nie, Y.F. Kuang, S.Z. Yao, *Carbon* 42 (2004) 191–197.
- [25] C. Guzman, Y. Verde, E. Bustos, F. Manriquez, I. Terol, L.G. Arriaga, G. Orozco, *ECS Trans.* 20 (2009) 413–423.
- [26] K. Saminathan, V. Kamavaram, V. Veedu, A.M. Kannan, *Int. J. Hydrogen Energy* 34 (2009) 3838–3844.
- [27] D. Santiago, G.G. Rodríguez-Calero, H. Rivera, D.A. Tryk, M.A. Scibioh, C.R. Cabrera, *J. Electrochem. Soc.* 157 (2010) F189–F195.
- [28] D.J. Guo, H.L. Li, *J. Electroanal. Chem.* 573 (2004) 197–202.
- [29] S. Sattayasamitsathit, A.M. O'Mahony, X. Xiao, S.M. Brozik, C.M. Washburn, D.R. Wheeler, J. Cha, D.B. Burckel, R. Polsky, J. Wang, *Electrochem. Commun.* 13 (2011) 856–860.
- [30] X. Chen, N. Li, K. Eckhard, L. Stoica, W. Xia, J. Assmann, M. Muhler, W. Schuhmann, *Electrochem. Commun.* 9 (2007) 1348–1354.
- [31] F. Ye, L. Chen, J. Li, J. Li, X. Wang, *Electrochem. Commun.* 10 (2008) 476–479.
- [32] B.G. Pollet, *Electrochem. Commun.* 11 (2009) 1445–1448.
- [33] B.G. Pollet, E.F. Valzer, O.J. Curnick, *Int. J. Hydrogen Energy* 36 (2011) 6248–6258.
- [34] O. Antoine, R. Durand, *Electrochem. Solid-State Lett.* 4 (2001) A55–A58.
- [35] S. Lertviriyapaisan, N. Tantavichet, *Int. J. Hydrogen Energy* 35 (2010) 10464–10471.
- [36] R. Woods, *J. Electroanal. Chem.* 49 (1974) 217–226.
- [37] J.P. Hoare, *J. Electrochem. Soc.* 121 (1974) 872–876.
- [38] J.P. Hoare, *J. Phys. Chem.* 79 (1975) 2175–2179.